Am J Physiol Gastrointest Liver Physiol 295: G784–G790, 2008.
First published August 21, 2008; doi:10.1152/ajpgi.90434.2008.

Lipopolysaccharide activates NF-κB by TLR4-Bcl10-dependent and independent pathways in colonic epithelial cells

Sumit Bhattacharyya,[1] Pradeep K. Dudeja,[1,2] and Joanne K. Tobacman[1,2]

[1]*Department of Medicine, University of Illinois at Chicago and* [2]*Jesse Brown Veterans Affairs Medical Center, Chicago, Illinois*

Submitted 15 July 2008; accepted in final form 14 August 2008

Bhattacharyya S, Dudeja PK, Tobacman JK. Lipopolysaccharide activates NF-κB by TLR4-Bcl10-dependent and independent pathways in colonic epithelial cells. *Am J Physiol Gastrointest Liver Physiol* 295: G784–G790, 2008. First published August 21, 2008; doi:10.1152/ajpgi.90434.2008.—In colonic epithelium, one of the pathways of lipopolysaccharide (LPS) activation of NF-κB and IL-8 is via Toll-like receptor (TLR)4, MyD88, IRAK1/4, and B-cell CLL/lymphoma 10 (Bcl10). However, this innate immune pathway accounts for only ~50% of the NF-κB activation, so additional mechanisms to explain the LPS-induced effects are required. In this report, we identify a second pathway of LPS-induced stimulation, mediated by reactive oxygen species (ROS), in human colonic epithelial tissue cells in tissue culture and in ex vivo mouse colonic tissue. Measurements of IL-8, KC, Bcl10, phospho-IκBα, nuclear NF-κB, and phosphorylated Hsp27 were performed by ELISA. The TLR4-Bcl10 pathway was inhibited by Bcl10 siRNA and in studies with colonic tissue from the TLR4-deficient mouse. The ROS pathway was inhibited by Tempol, a free radical scavenger, or by okadaic acid, an inhibitor of Hsp27 dephosphorylation by protein phosphatase 2A (PP2A). The ROS pathway was unaffected in the TLR4-deficient tissue or by silencing of Bcl10. The combination of exposure to the free radical scavenger Tempol and of TLR4 or Bcl10 suppression was required to completely inhibit the LPS-induced activation. The ROS pathway was associated with dephosphorylation of Hsp27. LPS appears to activate both the regulatory component of the IκBα-kinase (IKK) signalosome through Bcl10 interaction with Nemo (IKKγ) and the catalytic component through Hsp27 interaction with IKKβ. Since LPS exposure is associated with septic shock and the systemic inflammatory response syndrome, distinguishing between these two pathways of LPS activation may facilitate new approaches to prevention and treatment.

IKK signalosome; Bcl10; lipopolysaccharide; Hsp27; TLR4; reactive oxygen species

LIPOPOLYSACCHARIDE (LPS) from the bacterial cell wall induces inflammation in experimental models and is a significant source of clinical morbidity and mortality owing to its role in the etiology of systemic inflammatory response syndrome (SIRS) and sepsis. Although improvements in the therapeutic approach to SIRS and sepsis have been achieved, better understanding of the underlying mechanisms by which LPS induces inflammation may improve clinical outcomes and lead to new approaches to treatment. Recently, we reported that the LPS-Toll-like receptor (TLR)4-induced pathway of NF-κB activation in colonic epithelial cells required Bcl10 (B-cell CLL/lymphoma 10), a caspase-recruitment domain (CARD)-containing adaptor protein (5). Previously, translocations involving Bcl10 were associated with constitutive activation of NF-κB in the MALT (mucosa-associated lymphoid tumor) lymphomas and identified in the innate immune response cascade in lymphocytes and macrophages (9, 19, 28, 30, 31). Other recent reports have also identified Bcl10 as a mediator of an inflammatory cascade in nonimmune cells (16, 20, 26).

In the colonic epithelial cells, silencing Bcl10 by small-interfering RNA (siRNA) did not entirely inhibit LPS-activation of the phospho-IκBα-NF-κB-IL-8 cascade. In this report, we present a second pathway of LPS-induced activation of NF-κB that proceeds through increased reactive oxygen species (ROS) and reduced phosphorylated Hsp27 and is inhibited by the ROS scavenger Tempol. Bcl10 silencing by siRNA and exposure to Tempol together completely inhibited the LPS-induced activation of phospho-IκBα, NF-κB, and IL-8.

In addition to experiments with human colonic epithelial cells, we present data from experiments with macrophages and ex vivo colonic tissue from TLR4-deficient mice that support the occurrence of two distinct pathways of NF-κB activation initiated by LPS. Since Bcl10 interacts with IKKγ, the regulatory domain of the IKK signalosome, and Hsp27 phosphorylation is inversely associated with phosphorylation of IKKβ, a catalytic component of the IKK signalosome, the two pathways of LPS activation of NF-κB are likely to be integrated at the IKK signalosome (1, 15, 23, 24, 29). Recognition of these distinct mechanisms by which LPS activates the inflammatory response may facilitate the development of new therapeutic approaches.

MATERIALS AND METHODS

Cell culture of human colonic epithelial cells. The human colonic epithelial cell line NCM460 was originally derived from the normal mucosa of a 68-yr-old Hispanic man (21). For the experiments, NCM460 cells were grown in M3:10 media (INCELL, San Antonio, TX) at 37°C in a humidified, 5% CO_2 environment with media exchange at 2-day intervals in T25 flasks. Confluent cells were harvested by EDTA-trypsin and replated in multiwell tissue culture plates. In the majority of experiments, cells were treated with LPS (10 ng/ml) for 6 h. Cells were harvested by scraping, and total cell protein was measured by BCA protein assay kit (Pierce, Rockford, IL), with bovine serum albumin as standard. Spent media were collected from control and treated wells and stored at −80°C.

Ex vivo studies with TLR4-deficient mouse colon. Mice with a deletion of the TLR4 gene locus (C57BL/10ScNJ) as well as normal, age-matched controls (C57BL/10ScSnJ) were obtained from The Jackson Laboratory (Bar Harbor, ME) (13). Animal care was approved by the Institutional Animal Care and Use Committees of the University of Illinois at Chicago and the Jesse Brown Veterans Affairs

Address for reprint requests and other correspondence: J. K. Tobacman, Dept. of Medicine, Univ. of Illinois at Chicago, CSN 440, M/C 718, Chicago, IL 60612 (e-mail: jkt@uic.edu).

The costs of publication of this article were defrayed in part by the payment of page charges. The article must therefore be hereby marked "*advertisement*" in accordance with 18 U.S.C. Section 1734 solely to indicate this fact.

Medical Center. Mice were euthanized at 8 wk, and the colonic tissue was excised and placed in DMEM with 10% FBS and Pen-Strep antibiotics. Tissue was cut into small fragments 1 mm × 2 mm and placed into wells of a 24-well tissue culture plate. Triplicate samples with technical replicates were exposed to lipopolysaccharide (LPS) 1 ng/ml for 2 or 6 h, while incubated in a humidified environment at 37°C with 5% CO_2. Samples were also exposed to LPS in combination with Tempol (4-hydroxy-2,2,6,6-tetramethylpiperidinyloxy, 100 nM), a ROS quencher, or with okadaic acid (5 nM), an inhibitor of protein phosphatase 2A (PP2A) (8, 11). Tissue was incubated at 37°C and 5% CO_2. At 2 and 6 h, spent media were collected for measurement of KC, the murine homolog of IL-8, by ELISA. The treated control and TLR4-deficient tissues were collected and homogenized, and soluble lysates were prepared for the determination of Bcl10, phospho-IκBα, and phospho-Hsp27 by ELISA.

Measurement of ROS. The production of ROS following LPS exposure was measured by use of hydroethidine for detection (22). Hydroethidine (HE) detects intracellular superoxide anion by changing from blue to red fluorescence when the oxyethidium derivative forms in the presence of O_2^-. NCM460 cells were harvested from T-75 flasks and seeded in a 96-well tissue culture plate. After 24 h, the media were changed, and treatment with LPS and the free radical scavenger Tempol began. After 2 h or 6 h exposure, the media were removed, and cells were washed with Hank's balanced salt solution (HBSS). Cells were incubated at 37°C for 60 min with 200 μl HBSS containing 10 μM HE. Media were removed, and fresh HBSS (200 μl/well) added. Intracellular HE fluorescence emitted by the cells was measured using a microplate fluorescence reader (FL600, Bio-Tek Instruments) at 488-nm excitation with a 610-nm emission filter.

Silencing Bcl10 by siRNA. siRNA for Bcl10 (NCBI NM_003921) silencing and control, scrambled siRNA labeled with rhodamine were procured (Qiagen, Valencia, CA). The expression of Bcl10 was silenced in NCM460 colonic cells, as reported previously (5, 7). The effectiveness of Bcl10 silencing was determined by Western blot of the cell lysates with Bcl10 monoclonal antibody (Santa Cruz Biotechnology). Following exposure to siRNA for 24 h, cells were treated with LPS or LPS in combination with Tempol or okadaic acid.

Measurement of IL-8 secretion by ELISA. Secretion of IL-8 in the spent media of control and treated NCM460 cells was measured with the DuoSet ELISA kit for human IL-8 (R&D Systems), as described previously (4, 5). Sample values were normalized with total protein content (BCA protein assay; Pierce) and expressed as picograms per milligram cellular protein.

Measurement of KC secretion by ELISA. Ex vivo colon tissues from control and TLR-deficient mice were treated with LPS alone or in combination with Tempol or okadaic acid. Following exposure for 2 or 6 h, the spent medium was collected and secretion of KC in the media determined. KC was captured in microtiter wells coated with rat anti-mouse monoclonal antibody to KC. Captured KC molecules were detected by biotinylated goat anti-mouse KC antibody and streptavidin-horseradish peroxidase (HRP), and the enzyme activity of bound HRP was determined by adding hydrogen peroxide-tetramethylbenzidine (TMB) chromogenic substrate (R&D). The magnitude of the optical density of the developed color was measured in an ELISA plate reader at 450 nm. KC concentrations were determined from a standard curve made with known concentrations of KC. Sample values were normalized with the total protein concentrations determined by BCA protein assay kit (Pierce).

ELISA for Bcl10. The protein content of Bcl10 in the NCM460 cells was determined by a solid-phase sandwich ELISA designed to quantify cellular Bcl10, as previously reported (6). Control and treated ex vivo colon tissues of normal and TLR-deficient mice were homogenized, and lysates were prepared in RIPA buffer. Bcl10 was measured by ELISA using a goat polyclonal Bcl10 antibody against an NH_2-terminal epitope of Bcl10 as the capture antibody (Santa Cruz Biotechnology, Santa Cruz, CA). A mouse monoclonal Bcl10 antibody (Santa Cruz Biotechnology) and goat anti-mouse IgG-HRP were used for detection, with hydrogen peroxide/TMB for color development.

ELISA for phospho-IκBα. Phospho-IκBα in the control and treated cells NCM460 cells was measured by the PathScan Sandwich ELISA (Cell Signaling Technology, Danvers, MA) that detects IκBα with phosphorylation of Ser32. NCM460 cells were grown in 24-well plates and treated with LPS (10 ng/ml × 6 h), after treatment with control siRNA or Bcl10 siRNA for 24 h, either alone or in combination with Tempol. Ex vivo colonic tissues, prepared as indicated above from control and TLR-deficient mice, were treated with LPS alone or in combination with Tempol or okadaic acid. Following treatment, extracts were prepared from treated and control NCM460 cells and from homogenized treated and control ex vivo mouse colonic tissue. Lysates were prepared in ice-cold lysis buffer (Cell Signaling Technology) that contained 20 mM Tris, pH 7.5, 150 mM NaCl, 1 mM EDTA, 1 mM EGTA, 1% Triton X-100, 2.5 mM sodium pyrophosphate, 1 mM β-glycerophosphate, 1 mM Na_3VO_4, 1 μg/ml leupeptin, and 1 mM PMSF. Cells were sonicated twice for 20 s and centrifuged at 13,500 *g* for 10 min at 4°C. The supernatant (cell lysate) was collected and stored at −80°C until assayed. Phospho-IκBα in the samples was captured in microtiter wells that were coated with monoclonal antibody to IκBα. Captured IκBα was detected by a specific rabbit phospho-IκBα antibody that detected Ser32 phosphorylation and was then recognized by an anti-rabbit IgG-HRP. The enzyme activity of bound HRP was determined by adding hydrogen peroxide-TMB chromogenic substrate. The magnitude of the optical density for the developed color was measured in an ELISA reader at 450 nm, after stopping the reaction with 2 N sulfuric acid. The intensity of the developed color is proportionate to the quantity of phospho-IκBα in each sample. Sample values were normalized with the total cell protein and expressed as percent control.

ELISA of nuclear NF-κB. Nuclear extracts were prepared from the treated and control NCM460 cells using a nuclear extraction kit, and activated NF-κB was determined by oligonucleotide-based ELISA (Active Motif). Treated and control samples were incubated in 96-well microtiter wells that were coated with the NF-κB consensus nucleotide sequence (5′-GGGACTTTCC-3′). NF-κB from the samples that attached to the wells was then captured by antibody to NF-κB (p65) and detected by an anti-rabbit-HRP-conjugated IgG. Color developed with hydrogen peroxide/TMB chromogenic substrate and was proportional to the quantity of NF-κB in each sample. Specificity of the NF-κB binding to the nucleotide sequence was determined by adding either free consensus nucleotide or mutated nucleotide to the reaction buffer. The sample values were normalized with the total cell protein determined by protein assay kit (Pierce).

Measurement of phosphorylated Hsp27 by ELISA. Phospho-Hsp27 in the control and treated NCM460 cells was measured by ELISA (R&D). NCM460 cells were grown in 24 well plates and treated with LPS (10 ng/ml × 6 h), after treatment with control or Bcl10 siRNA, and either with or without Tempol or okadaic acid. Similarly, ex vivo colon tissues from control and TLR-deficient mice were treated with LPS alone or in combination with Tempol or okadaic acid. Following LPS exposure, extracts were prepared from treated and control NCM460 cells or homogenized treated and control ex vivo colonic tissue of mice and phospho-Hsp27 was measured. Phospho-Hsp27 was captured in microtiter wells coated with monoclonal antibody to Hsp27. Captured phospho-Hsp27 molecules were detected by an anti-phospho Hsp27 antibody conjugated with biotin and streptavidin-HRP and the enzyme activity of bound HRP was determined by adding hydrogen peroxide-TMB chromogenic substrate. The magnitude of the optical density for the developed color was measured in an ELISA reader at 450 nm, after the reaction was stopped. The intensity of the developed color is proportionate to the quantity of phospho-Hsp27 in each sample. Phospho-Hsp27 concentrations of the samples were extrapolated from a standard curve derived by using known concentrations of phospho-Hsp27. Sample values were normalized

with the total cell protein concentrations determined by BCA protein assay (Pierce).

Statistical analysis. Data are means ± SD of three biological samples with two technical replicates of each, unless stated otherwise. Statistical significance was determined in all of the experiments by one-way ANOVA followed by a post hoc Tukey-Kramer test for multiple comparisons using Prism or Instat software.

RESULTS

LPS-induced increase in ROS. Production of ROS in NCM460 cells was markedly increased, following exposure to LPS (10 ng/ml) at 1 and 6 h (Fig. 1). When treated with LPS, the ROS production in the NCM460 cells increased to over 10 times the control level within the first hour of treatment and to over 19 times the control level at 6 h. The differences between LPS-exposed and control cells were statistically significant at all time points (***$P < 0.001$).

When NCM460 cells were treated with LPS in the presence of the free radical scavenger Tempol, significant reduction in production of ROS occurred (Fig. 1) (***$P < 0.001$). In the presence of Tempol (100 nM for 1 or 6 h), ROS levels declined to less than baseline values.

LPS-induced increase in IL-8 secretion from NCM460 cells. LPS treatment resulted in a marked increase in IL-8 secretion from the NCM460 cells. This increase was blocked significantly (***$P < 0.001$), in the presence of Tempol (Fig. 2). Following LPS (10 ng/ml), IL-8 secretion rose from 27 ± 1 pg/mg protein to 430 ± 39 pg/mg protein within an hour and to 2,588 ± 91 pg/mg protein at 6 h.

In the presence of Tempol, IL-8 declined to 1,548 ± 48 pg/mg protein at 6 h, compared with a control value of 166 ± 9 pg/mg protein. Almost 43% of the LPS-associated increase in IL-8 was attributable to an effect of ROS.

LPS-induced increases in IL-8 secretion depend on both Bcl10 and ROS. NCM460 cells were treated with siRNA for Bcl10, Tempol, and LPS, as well as the appropriate controls, and the IL-8 concentrations in the spent media were measured. Both Bcl10 siRNA and Tempol were required to eliminate the LPS-induced increase in IL-8 (Fig. 3). Tempol reduced the LPS-induced increase in IL-8 less than Bcl10 silencing (from 2,584 ± 140 to 1,259 ± 35 pg/mg protein). Some of the Tempol-associated decline in IL-8 was attributable to a small effect on the baseline IL-8 secretion. Basal IL-8 secretion declined to 110 ± 5 pg/mg protein from 172 ± 9 pg/mg protein because of Tempol. These findings demonstrated that LPS-induced IL-8 secretion proceeds predominantly through the Bcl10-mediated pathway, with a secondary pathway through ROS.

Tempol did not affect the LPS-induced increase in Bcl10. NCM460 cells were treated with siRNA for Bcl10, Tempol, and LPS either alone or in different combinations, as well as the appropriate controls, and Bcl10 concentrations were determined. LPS increased the Bcl10 concentration in the cells, but Tempol, either alone or in combination with LPS, had no effect on Bcl10 concentration (Fig. 4). Hence, the LPS-induced ROS and IL-8 production do not involve Bcl10 signaling but influence IL-8 secretion by an independent pathway.

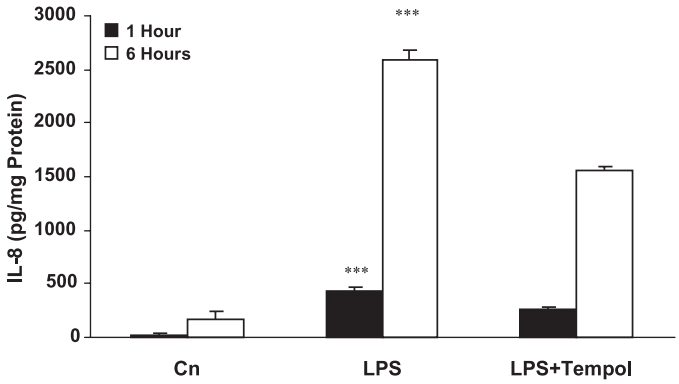

Fig. 2. Increased IL-8 secretion reduced by Tempol. IL-8 secretion from NCM460 cells was inhibited by Tempol when cells were treated with LPS (10 ng/ml) for 1 h or 6 h. LPS increased IL-8 secretion to 2,588 ± 91 pg/mg protein, but in the presence of Tempol IL-8 secretion declined to 1,548 ± 48 pg/mg protein. The increase with LPS exposure and the decline with Tempol were statistically significant at both time points (***$P < 0.001$).

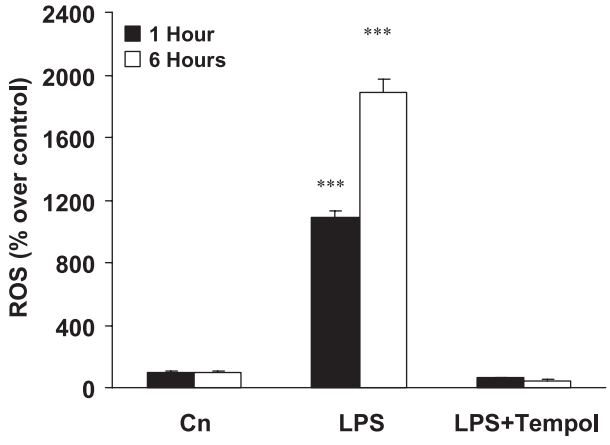

Fig. 1. Increased reactive oxygen species (ROS) production following LPS exposure in NCM460 cells. NCM460 cells in culture were treated with LPS (10 ng/ml) for 1 h or 6 h and ROS production was measured. LPS stimulated ROS production within 1 h. Differences between the control (Cn) and treated cells at the same time point are statistically significant (***$P < 0.001$). When NCM460 cells were treated with LPS in combination with Tempol 100 nM, the production of ROS declined to less than baseline (***$P < 0.001$).

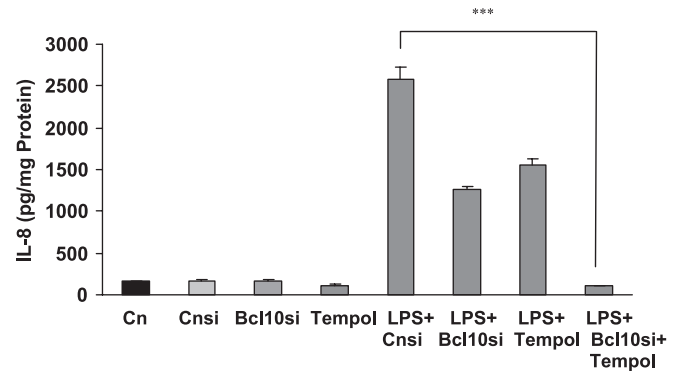

Fig. 3. Combination of Bcl10 silencing by small-interfering RNA (siRNA) and ROS quenching by Tempol required to inhibit LPS-induced increase in IL-8. The LPS-induced increase in secreted IL-8 was reduced to less than baseline by the combination of Tempol and Bcl10 silencing, but neither Tempol nor Bcl10 silencing alone was sufficient to inhibit the LPS-induced increase. Differences from control values following LPS and LPS with Bcl10 siRNA (Bcl10si) or LPS with Tempol or LPS with Bcl10 siRNA and Tempol were statistically significant (***$P < 0.001$). Cnsi, control siRNA.

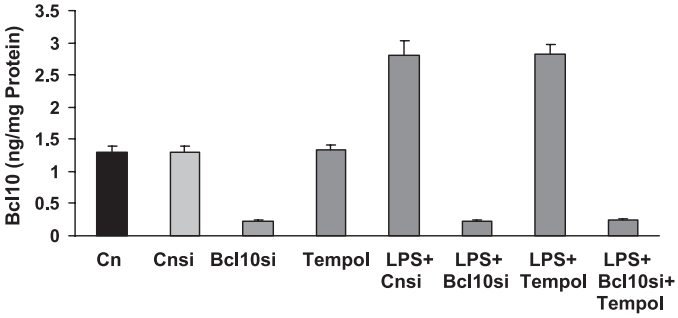

Fig. 4. Bcl10 content not reduced by Tempol. In the NCM460 cells, Bcl10 content was increased by LPS exposure, but Tempol had no effect on the Bcl10 content. No significant difference in Bcl10 was found between LPS + control siRNA and LPS + Tempol ($P > 0.05$).

ROS production associated with LPS-induced decline in phospho-Hsp27. Phospho-Hsp27 was measured by ELISA in control and LPS-treated NCM460 cells. Phospho-Hsp27 declined significantly (***$P < 0.001$) following LPS exposure (10 ng/ml × 6 h) (Fig. 5). Combined exposure to LPS and Tempol reversed the LPS-induced decline in phospho-Hsp27. In contrast, Bcl10 knockdown by siRNA had no effect on the LPS-induced reduction in phospho-Hsp27. Exposure to Tempol alone increased the baseline phospho-Hsp27 by 44 ± 5%. LPS alone reduced the phospho-Hsp27 by 56 ± 2%, but in combination with Tempol it increased the value by 42 ± 7% over the baseline. These results demonstrated that the LPS-induced increase in ROS production was responsible for the decline in phospho-Hsp27, since the decline was reversed by the addition of an ROS scavenger. In contrast, Bcl10 silencing had no effect on phospho-Hsp27. Differences observed between control and LPS and control and Tempol groups are statistically significant (***$P < 0.001$).

LPS-induced increases in phosphorylation of IκBα and activation of NF-κB depend on both Bcl10 and ROS. NCM460 cells were treated with siRNA for Bcl10, Tempol, and LPS, alone or in combination, and the phospho-IκBα and activated NF-κB (p65) content were measured. Both Tempol and Bcl10 siRNA were required to inhibit the LPS-induced increase in phospho-IκBα and nuclear NF-κB. Transfection of control cells with only Bcl10 siRNA had no effect on phospho-IκBα. In contrast, Tempol alone reduced the baseline phospho-IκBα 20 ± 6%. LPS exposure increased both the phospho-IκBα (Fig. 6*A*) and activated NF-κB (Fig. 6*B*) to ~300% of the baseline level. Bcl10 silencing decreased the LPS-induced activation by ~66% and Tempol reduced it by ~45–50%. Bcl10 silencing and Tempol in combination totally inhibited the LPS-induced increases in the phosphorylation of IκBα and activation of NF-κB. These data suggest that LPS stimulates the phosphorylation of IκBα and the activation of NF-κB through two distinct signaling pathways.

Effect of Bcl10 silencing on KC in TLR4-deficient mouse macrophages. To determine whether there were any alternate pathway involving Bcl10 that did not require TLR4, we tested the effect of LPS stimulation on KC in TLR4-deficient mouse macrophages following Bcl10 silencing by siRNA (Fig. 7). The increase in KC was much greater in the control mouse macrophages (2,603 ± 78 vs. 1,264 ± 111 pg/mg protein from baseline values of 305 ± 19 and 319 ± 6 pg/mg protein). Bcl10 silencing produced a decline in KC response in the control macrophages but had no effect in the TLR4-deficient cells, consistent with TLR4 and Bcl10 mediating the same path to chemokine activation.

KC secretion from ex vivo colonic tissue of TLR4-deficient mice. Ex vivo colonic tissues from TLR4-deficient mice and normal control mice were treated with LPS alone or in com-

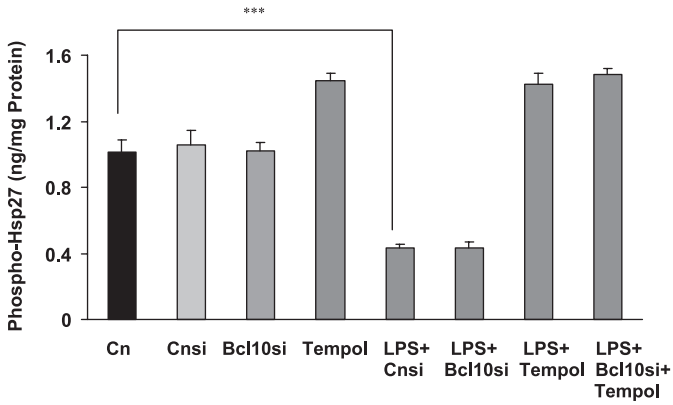

Fig. 5. Phospho-Hsp27 reduced by LPS, and unaffected by Bcl10 silencing. LPS reduced and Tempol increased the phospho-Hsp27 in the NCM460 cells (***$P < 0.001$). Tempol increased the phospho-Hsp27 by 40%, and LPS reduced the phospho-Hsp27 to 45% of baseline. Bcl10 silencing by siRNA had no impact on the phospho-Hsp27.

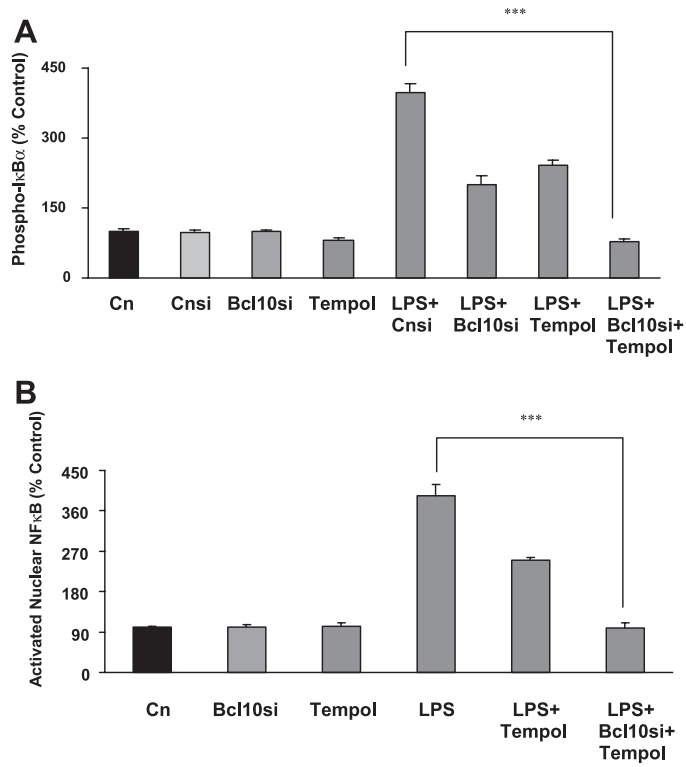

Fig. 6. Combined Bcl10 knockdown and ROS quenching by Tempol required to inhibit the LPS-induced increases in phospho-IκBα and NF-κB. LPS-induced increases in phospho-IκBα (*A*) and nuclear NF-κB (p65) (*B*) were reduced to less than baseline by the combination of Tempol and Bcl10 silencing, but neither Tempol nor Bcl10 silencing alone was sufficient to inhibit the LPS-induced increases. Differences between values following LPS and LPS with Bcl10 siRNA or LPS with Tempol or LPS with Tempol and Bcl10 siRNA are statistically significant (***$P < 0.001$).

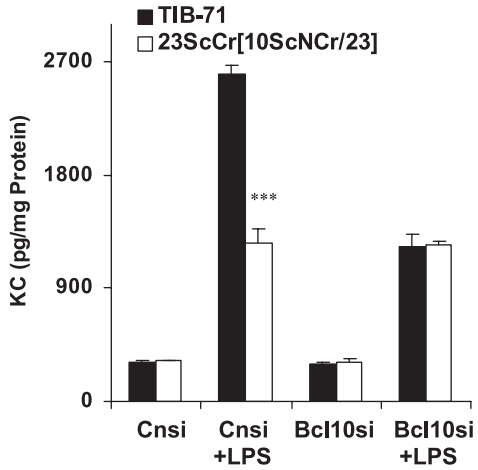

Fig. 7. In TLR4-deficient models, no effect of Bcl10 silencing on KC. LPS increased the KC secretion from 305 ± 18 pg/mg protein to 2,603 ± 78 pg/mg protein in the control TIB-71 macrophages. With Bcl10 knockdown by siRNA, KC decreased to 1,231 ± 98 pg/mg protein. In the TLR4-deficient macrophages (23ScCr), LPS increased the KC secretion less, from 319 ± 6 pg/mg protein to 1,264 ± 111 pg/mg protein (***$P < 0.001$) and was unaffected by Bcl10 silencing.

bination with Tempol or okadaic acid. At the end of the treatment, the spent media were collected and assayed for KC, the murine IL-8 homolog. Tissues were homogenized and solubilized in lysis buffer, and phospho-Hsp27, phospho-IκBα, and Bcl10 were measured by ELISA.

LPS treatment (1 ng/ml × 6 h) increased the KC secretion from baseline value of 251 ± 19 to 373 ± 31 pg/mg protein in the ex vivo TLR4-deficient colonic tissue. In the control tissue, LPS induced an increase from 250 ± 13 to 582 ± 17 pg/mg protein (Fig. 8*A*). The absence of the TLR4 receptor markedly reduced the LPS effect. The increase in KC secretion was totally inhibited in the TLR4-deficient mice by either Tempol or okadaic acid, two inhibitors of the ROS pathway. In contrast, similar treatment inhibited the LPS-induced increase in KC secretion in the control mice by only ~55%, since neither Tempol nor okadaic acid inhibit the TLR4-Bcl10 pathway.

Effect of LPS on phospho-Hsp27 in TLR4-deficient mouse. Determinations of phospho-Hsp27 (Fig. 8*B*) in ex vivo colonic tissue from TLR4-deficient and control mice were performed following treatment with LPS, either alone or in combination with Tempol or okadaic acid. LPS reduced the phospho-Hsp27 to 0.47 ± 0.05 from 1.04 ± 0.08 ng/mg protein, 45% of the baseline control value. Tempol and okadaic acid alone increased the phospho-Hsp27 concentration to 122–125% of the baseline level. In the TLR4-deficient and in the control mice, the effects of Tempol or okadaic acid and LPS with Tempol or okadaic acid on phospho-Hsp27 were similar.

Effect of LPS on phospho-IκBα in TLR4-deficient mouse. In the TLR4-deficient mouse colonic tissue, LPS increased the phospho-IκBα concentration by 54 ± 9% and increased the phospho-IκBα concentration by 154 ± 22% in the control

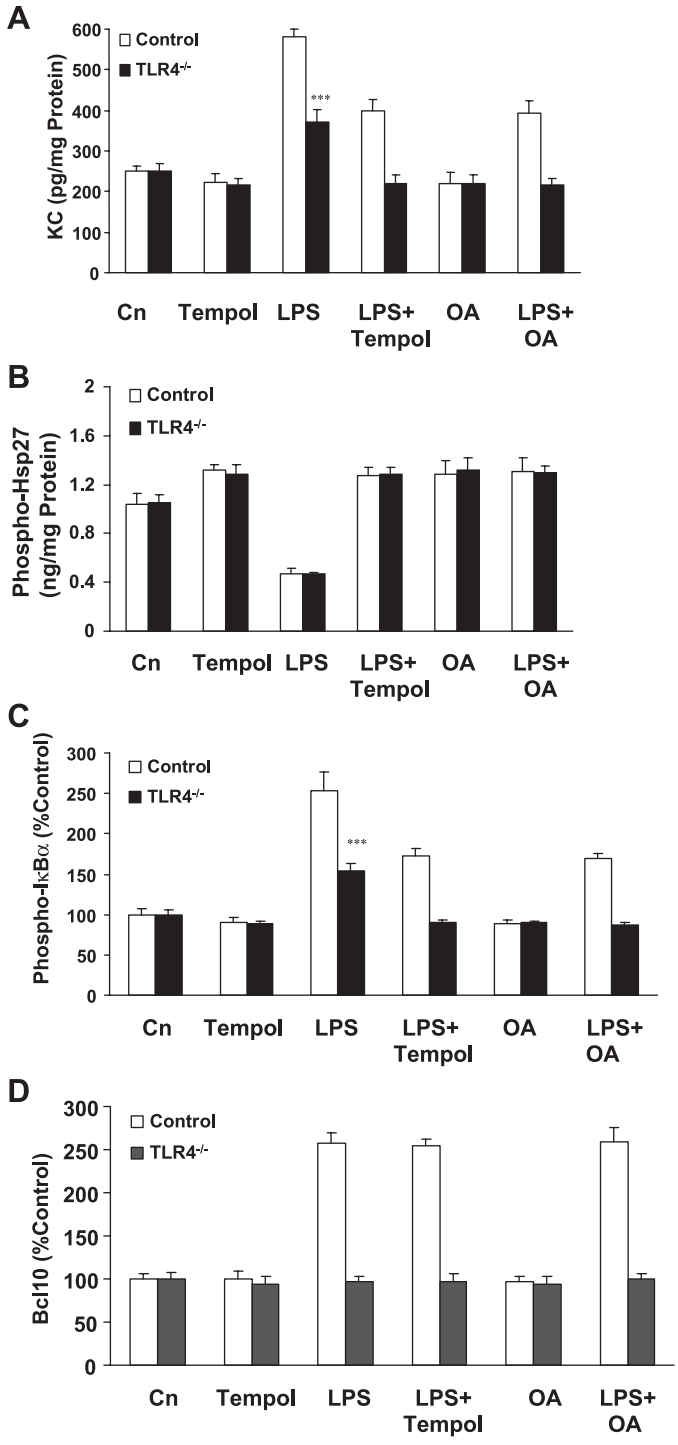

Fig. 8. Measurements of KC, phospho-Hsp27, and phospho-IκBα from ex vivo colonic tissue of TLR4-deficient and control mice. Ex vivo colonic tissue from TLR4-deficient and control mice were treated with LPS 1 ng/ml alone or in combination with Tempol 100 nM or okadaic acid (OA) 25 nM for 6 h. LPS-induced increase in KC secretion was significantly greater in the control than the TLR4-deficient colonic tissue (***$P < 0.001$). Tempol and okadaic acid reduced the response to KC in both the TLR4-deficient and control samples (*A*). In the TLR4-deficient mouse colonic tissue, the changes in phospho-Hsp27 content were similar to those in the control tissue. Tempol and okadaic acid inhibited the LPS-induced decline in phospho-Hsp27 (*B*). The increase in phospho-IκBα concentration following LPS exposure was greater in the control than in the TLR4-deficient mouse colonic tissue (***$P < 0.001$) (*C*). Tempol and okadaic acid had similar effects on reduction of the phospho-IκBα content in the TLR4-deficient and control samples. When Bcl10 content was measured in ex vivo colonic tissue from TLR4-deficient and control mice following LPS (1 ng/ml × 6 h), no increase in the Bcl10 content was demonstrated in the TLR4-deficient tissue, in contrast to a significant increase in the control sample (*D*).

mice (Fig. 8*C*). The increase in phospho-IκBα was totally nullified by cotreatment with Tempol or okadaic acid in the TLR4-deficient mouse, consistent with ROS mediation of only the LPS-induced pathway of NF-κB activation in the TLR4-deficient mouse tissue. Tempol and okadaic acid reduced the baseline phospho-IκBα concentration to less than baseline in the control and TLR4-deficient mice.

Bcl10 content in TLR4-deficient mouse. In the TLR4-deficient mice, neither LPS alone nor LPS in combination with Tempol or okadaic acid affected the Bcl10 concentration in the colonic tissue (Fig. 8*D*). In the control mouse tissue, LPS increased the Bcl10 concentration, but this increase was not affected by either Tempol or okadaic acid because they are inhibitors in the LPS-ROS pathway and have no effect on Bcl10.

DISCUSSION

Investigation of the mechanisms by which LPS activates NF-κB reveals that two distinct pathways are involved: a TLR4-Bcl10 pathway and an ROS-Hsp27 pathway (Fig. 9). These cascades are integrated at the level of the IKK signalosome, leading to the regulated phosphorylation of IκBα that enables the nuclear translocation of NF-κB (p65). Findings demonstrate that LPS stimulated both of these pathways in the human and mouse tissues studied and that the complete abrogation of NF-κB activation requires inhibition of both cascades.

In the TLR4-deficient mouse macrophages and ex vivo colonic tissue, LPS effects were mediated only by ROS, as demonstrated by the inhibitory effects of Tempol and okadaic acid on the LPS-induced increases in phospho-IκBα, NF-κB, and KC. The LPS-induced decline in phospho-Hsp27 was preserved in the TLR4-deficient colonic tissue, consistent with an intact ROS-mediated cascade. In the TLR4-deficient macrophages, KC secretion was less than in the control macrophages and was unaffected by Bcl10 silencing, consistent with absence of activation of the TLR4-Bcl10-mediated pathway. In contrast to the control tissue, Bcl10 silencing had no impact on phospho-IκBα, NF-κB, or KC in the TLR4-deficient ex vivo mouse colonic tissue. Bcl10 content did not increase following LPS exposure in the absence of TLR4. The combination of Bcl10 silencing and Tempol was required to completely inhibit the LPS-induced effects in the NCM460 cells.

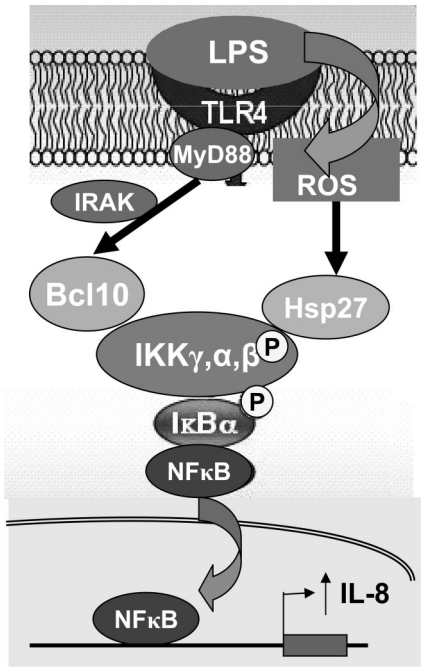

Fig. 9. Proposed model of LPS-induced activation of NF-κB-IL-8 through TLR4-MyD88-IRAK-Bcl10 and ROS-Hsp27 mediated pathways. The schematic drawing indicates 2 pathways of LPS-induced inflammation that appear to be integrated at the level of the IKK signalosome.

Integration of these distinct pathways of NF-κB activation at the level of the IKK signalosome is suggested by Bcl10's known interaction with IKKγ (Nemo), the regulatory component of the IKK signalosome, and by phospho-Hsp27's known inverse relationship with phospho-IKKβ (15, 23, 24, 29, 31). Bcl10 coimmunoprecipitates with IKKγ and influences its ubiquitination, which, in turn, affects the activation and ubiquitination of phospho-IκBα and produces the constitutive activation of NF-κB. The phosphorylation of Hsp27 is inverse to the phosphorylation of IKKβ, both of which can be dephosphorylated by PP2A. Study data demonstrate that the LPS-induced decline in phospho-Hsp27 was reversed by exposure to okadaic acid, an inhibitor of PP2A, or by the ROS scavenger Tempol. In contrast, Bcl10 siRNA had no impact on phospho-Hsp27. In the study experiments, we have not isolated specific changes in IKKβ, anticipating further work to investigate the phospho-exchanges involved.

The specific characteristics of LPS that lead to the TLR4-MyD88-IRAK-Bcl10-IKKγ or the ROS-Hsp27-IKKβ route of NF-κB activation require further clarification. LPS is a highly complex structure, including the conserved hydrophobic lipid A, the core oligosaccharide that is attached to lipid A, and the O-antigen, the variable polysaccharide side chain extending from the core oligosaccharide. The TLRs are able to recognize the pathogen-associated molecular pattern of LPS produced by bacteria or other pathogens and trigger the innate immune response (1). Other endogenous factors, including MD-2 and the lipoprotein receptor, may be required for interaction with TLR4 (18, 25). We have reported that the sulfated polysaccharide carrageenan, which has the unusual α-1,3-galactosidic link that is the epitope for the anti-Gal antibody (2, 12), is recognized by TLR4 and induces an innate immune response mediated by Bcl10, as well as an ROS-mediated inflammatory response (3, 4). The O-antigen of enteropathogenic *Escherichia coli* O86 and O127 appears to have some similarly configured linkages between galactose and *N*-acetylgalactosamine residues (10), suggesting a possible relationship to pathogenicity. Activation of the ROS pathway is expected to be initiated by interactions with membrane lipids. These reactions generate free radicals and stimulate a cascade that may include other mediators often implicated in LPS-induced inflammation (14, 17, 27). The ROS-induced cascade appears to culminate in the decline in Hsp27 phosphorylation and increase in IKKβ-IκBα phosphorylation.

This analysis presents two pathways by which LPS activates NF-κB and the IL-8 chemokine response. Separation of the LPS-induced effects into these two distinct pathways may facilitate the development of more highly specified interventions that reduce the morbidity and mortality associated with LPS-associated SIRS or septic shock. The LPS induction of

other mediators of the inflammatory cascade is not explained by the mechanisms elucidated in this report. Activation of multiple signaling mediators may be triggered by secondary effects initiated by LPS, including NF-κB and Bcl10 transcriptional effects in the epithelial cells and recruitment of a neutrophil and macrophage inflammatory infiltrate induced by IL-8 secretion.

REFERENCES

1. **Akira S, Uematsu S, Takeuchi O.** Pathogen recognition and innate immunity. *Cell* 124: 783–801, 2006.
2. **Baumann BC, Stussi G, Huggel K, Rieben R, Seebach JD.** Reactivity of human natural antibodies to endothelial cells from Galpha(1,3)Gal-deficient pigs. *Transplantation* 83: 193–201, 2007.
3. **Bhattacharyya S, Dudeja PK, Tobacman JK.** Carrageenan-induced NFkappaB activation depends on distinct pathways mediated by reactive oxygen species and Hsp27 or by Bcl10. *Biochim Biophys Acta* 1780: 973–982, 2008.
4. **Bhattacharyya S, Gill R, Chen ML, Zhang F, Linhardt RJ, Dudeja PK, Tobacman JK.** Toll-like receptor 4 mediates induction of Bcl10-NFκB-IL-8 inflammatory pathway by carrageenan in human intestinal epithelial cells. *J Biol Chem* 283: 10550–10558, 2008.
5. **Bhattacharyya S, Borthakur A, Pant N, Dudeja PK, Tobacman JK.** BCL-10 induces lipopolysaccharide induced activation of NFκB and IL-8 in human intestinal epithelial cells. *Am J Physiol Gastrointest Liver Physiol* 293: G429–G437, 2007.
6. **Bhattacharyya S, Pant N, Dudeja PK, Tobacman JK.** Development, evaluation, and application of a highly sensitive microtiter plate ELISA for human Bcl10 protein. *J Immunoassay Immunochem* 28: 173–188, 2007.
7. **Borthakur A, Bhattacharyya S, Dudeja PK, Tobacman JK.** Carrageenan induces interleukin-8 production through distinct Bcl10 pathway in normal human colonic epithelial cells. *Am J Physiol Gastrointest Liver Physiol* 292: G829–G838, 2007.
8. **Cuzzocrea S, McDonald MC, Mazzon E, Dugo L, Lepore V, Flonti MT, Ciccolo A, Terranova ML, Caputi AP, Thiemermann C.** Tempol, a membrane-permeable radical scavenger, reduces dinitrobenzene sulfonic acid-induced colitis. *Eur J Pharmacol* 406: 127–137, 2000.
9. **Dong W, Liu Y, Peng J, Chen L, Zou T, Xiao H, Liu Z, Li W, Bu Y, Qi Y.** The IRAK-1-Bcl10-MALT1-TRAF6-TAK1 cascade mediates signaling to NFκB from Toll-like receptor 4. *J Biol Chem* 281: 26029–26040, 2006.
10. **Feng L, Han W, Wang Q, Bastin D, Wang L.** Characterization of Escherichia coli O86 O-antigen gene cluster and identification of O86-specific genes. *Vet Microbiol* 106: 241–248, 2005.
11. **Forsyth CJ, Sabes SF, Urbanek RA.** An efficient total synthesis of okadaic acid. *J Am Chem Soc* 119: 8381–8382, 1997.
12. **Galili U.** The alpha-gal epitope and the anti-Gal antibody in xenotransplantation and in cancer immunotherapy. *Immunol Cell Biol* 83: 674–686, 2005.
13. **Hornef MM, Frisan T, Vandewalle A, Normark S, Richter-Dahlfors A.** Toll-like receptor 4 resides in the Golgi apparatus and colocalizes with internalized lipopolysaccharide in intestinal epithelial cells. *J Exp Med* 195: 559–570, 2002.
14. **Jang S, Kelley KW, Johnson RW.** Luteolin reduces IL-6 production in microglia by inhibiting JNK phosphorylation and activation of AP-1. *Proc Natl Acad Sci USA* 105: 7534–7539, 2008.
15. **Kammanadiminti SJ, Chadee K.** Suppression of NF-kappaB activation by Entamoeba histolytica in intestinal epithelial cells is mediated by heat shock protein 27. *J Biol Chem* 281: 26112–26120, 2006.
16. **Klemm S, Zimmermann S, Peschel C, Mak TW, Ruland J.** Bcl10 and Malt1 control lysophosphatidic acid-induced NFkappaB activation and cytokine production. *Proc Natl Acad Sci USA* 104: 134–138, 2007.
17. **Lee SA, Park SH, Kim BC.** Raloxifene, a selective estrogen receptor modulator, inhibits lipopolysaccharide-induced nitric oxide production by inhibiting the phosphatidylinositol 3-kinase/Akt/nuclear factor-kappa B pathway in RAW264.7 macrophage cells. *Mol Cells* 26: 48–52, 2008.
18. **Lenoir C, Sapin C, Broquet AH, Jouniaux AM, Bardin S, Gasnereau I, Thomas G, Seksik P, Trugnan G, Masliah J, Bachelet M.** MD-2 controls bacterial lipopolysaccharide hyporesponsiveness in human intestinal epithelial cells. *Life Sci* 82: 519–528, 2008.
19. **Lucas PC, Yonequmi M, Inohara N.** Bcl10 and MALT1 independent targets of chromosomal translocation in Malt lymphoma cooperate in a novel NFkappaB signaling pathway. *J Biol Chem* 276: 19012–19019, 2001.
20. **McAllister-Lucas LM, Ruland J, Siu K, Jin X, Gu S, Kim DS, Kuffa P, Kohrt D, Mak TW, Nuñez G, Lucas PC.** CARMA3/Bcl10/MALT1-dependent NFkappaB activation mediates angiotensin II-responsive inflammatory signaling in nonimmune cells. *Proc Natl Acad Sci USA* 104: 139–144, 2007.
21. **Moyer MP, Manzano LA, Merriman RL, Stauffer JS, Tanzer LR.** NCM460, a normal human colon mucosal epithelial cell line. *In Vitro Cell Dev Biol Anim* 32: 315–317, 1996.
22. **Ndengele MM, Muscoli CW, Wang ZQ, Doyle TM, Matuschak GM, Salvemini D.** Superoxide potentiates NFκB activation and modulates endotoxin-induced cytokine production in alveolar macrophages. *Shock* 23: 186–193, 2005.
23. **Park KJ, Gaynor RB, Kwak YT.** Heat shock protein 27 association with the I kappa B kinase complex regulates tumor necrosis factor alpha-induced NF-kappa B activation. *J Biol Chem* 278: 35272–35278, 2003.
24. **Sur R, Lyte PA, Southall MD.** Hsp27 regulates pro-inflammatory mediator release in keratinocytes by modulating NF-kappaB signaling. *J Invest Dermatol* 128: 1116–1122, 2008.
25. **Vasl J, Prohinar P, Gioannini TL, Weiss JP, Jerala R.** Functional activity of MD-2 polymorphic variant is significantly different in soluble and TLR4-bound forms: decreased endotoxin binding by G56R MD-2 and its rescue by TLR4 ectodomain. *J Immunol* 180: 6107–6115, 2008.
26. **Wang D, You Y, Lin PC, Xue L, Morris SW, Zeng H, Wen R, Lin X.** Bcl10 plays a critical role in NF-κB activation induced by G protein-coupled receptors. *Proc Natl Acad Sci USA* 104: 145–150, 2007.
27. **Wang X, Xue H, Xu Q, Zhang K, Hao X, Wang L, Yan G.** p38 kinase/cytosolic phospholipase A(2)/cyclooxygenase-2 pathway: A new signaling cascade for lipopolysaccharide-induced interleukin-1beta and interleukin-6 release in differentiated U937 cells. *Prostaglandins Other Lipid Mediat* 86: 61–67, 2008.
28. **Willis TG, Jadayel DM, Du MQ, Peng H, Perry AR, Abdul-Rauf M, Price H, Karran L, Majekodunmi O, Wlodarska I, Pan L, Crook T, Hamoudi R, Isaacson PG, Dyer MJ.** Bcl10 is involved in t(1;14)(p22;q32) of MALT B Cell lymphoma and mutated in multiple tumor types. *Cell* 96: 46–56, 1999.
29. **Wu CJ, Ashwell JD.** Nemo recognition of ubiquitinated Bcl10 is required for T-cell receptor mediated NFkappaB activation. *Proc Natl Acad Sci USA* 105: 3023–3028, 2008.
30. **Zhang Q, Siebert R, Yan M, Hinzmann B, Cui X, Xue L, Rakestraw KM, Naeve CW, Beckmann G, Weisenburger DD, Sanger WG, Nowotny H, Vesely M, Callet-Bauchu E, Salles G, Dixit VM, Rosenthal A, Schlegelberger S, Morris SW.** Inactivating mutations and overexpression of Bcl10, a caspase recruitment domain-containing gene, in MALT lymphoma with t(1;14)(p22;q32). *Nat Genet* 22: 63–68, 1999.
31. **Zhou H, Wertz I, O'Rourke K, Ultsch M, Seshagiri S, Eby M, Xiao W, Dixit VM.** Bcl10 activates the NFκB pathway through ubiquitination of NEMO. *Nature* 427: 167–171, 2004.